

Synthesis, chemical ordering, and magnetic properties of FePtCu nanoparticle films

Xiangcheng Sun, Shishou Kang, J. W. Harrell, and David E. Nikles^{a)}

Center for Materials for Information Technology, The University of Alabama, Tuscaloosa, Alabama 35487-0209

Z. R. Dai, J. Li, and Z. L. Wang

School of Materials Science and Engineering, Georgia Institute of Technology, Atlanta, Georgia 30332-0245

(Presented on 13 November 2002)

FePtCu nanoparticles with varying composition were prepared by the simultaneous polyol reduction of platinum acetylacetonate and copper bis(2,2,6,6-tetramethyl-3,5-heptanedionate) and the thermal decomposition of iron pentacarbonyl. As prepared the particles had a fcc structure with an average diameter of 3.5 nm and were superparamagnetic. Heat treatment of the self-assembled films at temperatures above 550 °C transformed the particles from the fcc to the $L1_0$ phase, give in-plane coercivities as high as 9000 Oe. X-ray diffraction revealed that the Cu remained in the films and the presence of an extra peak, indicating a second phase was present. Consistent with two or more phases, the magnetic hysteresis curves could be decomposed into a hard component ($H_c > 5000$ Oe) and a soft component ($H_c < 2000$ Oe). Unlike our earlier results for Ag in FePt, adding Cu to FePt did not lower the temperature required for phase transformation from the fcc to the $L1_0$ phase. © 2003 American Institute of Physics. [DOI: 10.1063/1.1543863]

INTRODUCTION

The report by Sun *et al.*¹ on the synthesis, self-assembly and magnetic properties of nanometer-sized FePt particles caused an explosion of interest in the use of these particles in granular magnetic recording media. Films containing self-assembled FePt nanoparticles must be heat-treated at temperatures above 550 °C to transform the particles to the $L1_0$ phase having high magnetocrystalline anisotropy.² However, there was considerable particle coalescence and loss of particle positional order when the films were heated to temperatures above 550 °C.³ Particle coalescence leads to increased switching volumes and increases the distribution of particle volumes, which defeats the objective of making small monodisperse nanoparticles. The loss of positional order came from the decomposition of the surfactant layers thereby allowing particle motion. It would be highly desirable if the temperature required for the fcc to tetragonal phase transformation were lower, at least below temperatures where the particles coalesce, preferably below the temperature where the organic surfactants decompose.

Maeda *et al.* observed that adding copper into FePt sputtered films greatly reduced the ordering temperature.⁴ For films containing $[\text{FePt}]_{85}\text{Cu}_{15}$ the coercivity was 5000 Oe after annealing at 300 °C, while H_c for films containing FePt was only a few hundred Oe after annealing at 300 °C. Takahashi and co-workers found that adding 4 at. % Cu into FePt sputtered films decreased the temperature required for fcc to $L1_0$ ordering from 500 to 400 °C.⁵ They suggested that the addition of Cu lowered the melting point for the alloy, increasing the atomic diffusivity, thereby enhancing the kinet-

ics of ordering. These reports suggest the possibility of lowering the temperature needed to bring about the fcc to $L1_0$ phase transformation for FePt nanoparticles by adding copper. Accordingly we set about the task of preparing FePt nanoparticles containing Cu. Unlike sputtered thin films using a Cu target, a suitable chemical procedure had to be found for introducing Cu into FePt. Here we report on the synthesis of FePtCu nanoparticles and the effect of the added copper on the phase transformation temperature.

EXPERIMENT

All chemicals were purchased from Aldrich Chemical Company and used as received. The particle composition was determined by energy dispersive x-ray analysis on a Philips model XL 30 scanning electron microscope. X-ray diffraction (XRD) data were obtained on a Rigaku D/MAX-2BX horizontal (XRD) thin film diffractometer using $\text{Cu } K\alpha$ radiation alpha transmission electron microscopy. (TEM) and high resolution TEM images were obtained on a Hitachi HF-2000 FE field emission at 200 keV and JEOL-4000 EX at 400 keV TEM. Magnetic hysteresis loops were measured with a Princeton Measurements Model 2900 alternating gradient magnetometer (AGM) with a maximum field of 20 kOe.

The synthesis of $\text{Fe}_{45}\text{Pt}_{44}\text{Cu}_{11}$ nanoparticles: A 50 mL three-necked round bottom flask was equipped with magnetic stirring, a reflux condenser, a thermometer, a rubber septum, magnetic stirring, and an argon atmosphere. Teflon sleeves were used for all ground glass joints. To the flask was added 0.25 mmol platinum acetylacetonate, 0.08 mmol copper bis(2,2,6,6-tetramethyl-3,5-heptanedionate), and 10 mL phenyl ether. The mixture was heated to 80 °C, whereupon it turned brown. Then 0.50 mmol oleic acid, 0.50 mmol oleyl

^{a)} Author to whom correspondence should be addressed; electronic mail: dnikles@mint.ua.edu

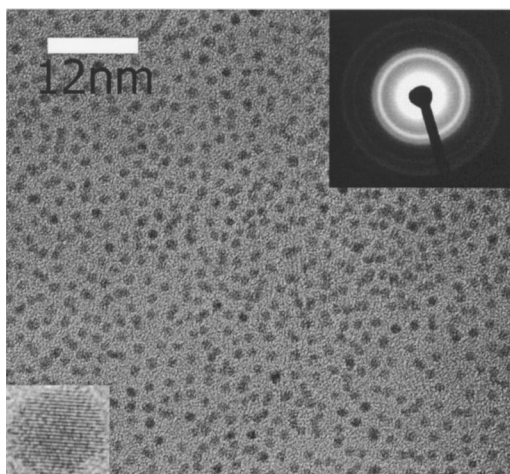


FIG. 1. TEM image of the FePtCu nanoparticles. The upper right inset is the selected area electron diffraction, while the lower left inset is a high resolution TEM image showing the lattice fringes.

amine, and 0.1 mL (0.08 mmol) iron pentacarbonyl were added by syringe. The septum was replaced with a glass stopper and the reaction mixture heated to the reflux temperature of phenyl ether ($\sim 260^\circ\text{C}$). After refluxing for 30 min, the reaction mixture was allowed to cool to room temperature, giving a dark dispersion. Ethanol (25 mL) was added to precipitate the particles and the particles were isolated by centrifuging. The particles were redispersed in hexane, precipitated with ethanol, and isolated by centrifuging. The particles were dispersed in a 50/50 mixture of hexane and octane, the dispersion cast onto either a silicon wafer or a carbon-coated TEM grid, and the solvent was allowed to evaporate at room temperature. The films were heat treated in a Lindberg tube furnace for 30 min in flowing 5% hydrogen in argon atmosphere.

RESULTS AND DISCUSSION

FePtCu nanoparticles were prepared by the simultaneous polyol reduction of platinum acetylacetonate and copper bis(2,2,6,6-tetramethyl-3,5-heptanedionate), and the thermal decomposition of iron pentacarbonyl in diphenyl ether solution. Initial attempts to prepare FePtCu nanoparticles using copper acetylacetonate in dioctyl ether met limited success. FePt nanoparticles containing small amounts of copper were prepared, however the limited solubility of $\text{Cu}(\text{acac})_2$ in dioctyl ether limited the amount of copper that could be incorporated into the particles. Copper bis(2,2,6,6-tetramethyl-3,5-heptanedionate) was quite soluble in diphenyl ether, allowing great freedom to vary the copper content in the particles. In fact, the relative amounts of iron, platinum, and copper in the particles depended on the amount of iron, platinum, and copper charged to the reaction.

The synthesis, dispersion, and self assembly of the FePtCu nanoparticles was exactly what one would expect based on previous experience with FePt, FeCoPt,⁶ or $[\text{Fe}_{49}\text{Pt}_{51}]_{88}\text{Ag}_{12}$ ⁷ nanoparticles. In Fig. 1 is a low magnification TEM image of the particles, as prepared, showing the average particle size was about 3.5 nm in diameter. The inset selected area electron diffraction pattern in Fig. 1 and the

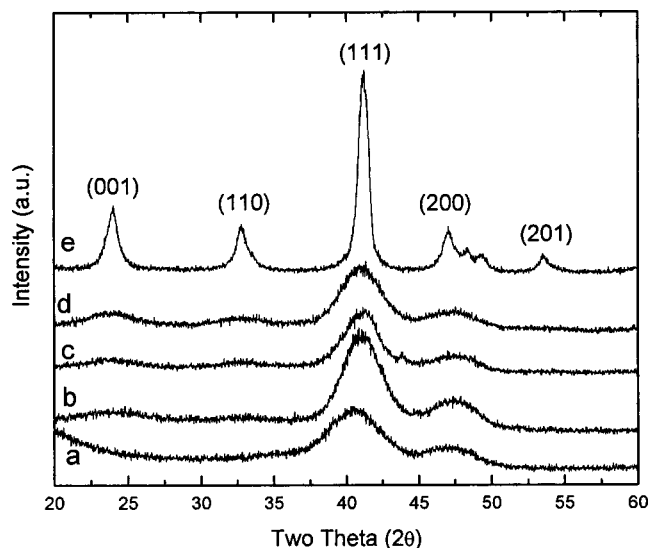


FIG. 2. X-ray diffraction curves for $\text{Fe}_{45}\text{Pt}_{44}\text{Cu}_{11}$; as-prepared, curve a; 500 °C, curve b; 550 °C, curve c; 600 °C, curve d; and 700 °C, curve e.

x-ray diffraction in Fig. 2 show the particles had a fcc structure. The lattice fringes in the high resolution TEM image inset in Fig. 1 shows that the particles are single crystal fcc.

The films were heat treated in a tube furnace under flowing 5% hydrogen in argon for 30 min. The purpose of the hydrogen was to avoid oxidation. Unlike the case with films containing $[\text{Fe}_{49}\text{Pt}_{51}]_{88}\text{Ag}_{12}$ nanoparticles⁷ or with FePt sputtered films containing Cu, to our dismay, there was no decrease in the temperature required to transform the FePtCu nanoparticles from the fcc phase to the $L1_0$ phase. In Fig. 2 are a series of XRD curves for films containing $\text{Fe}_{45}\text{Pt}_{44}\text{Cu}_{11}$ nanoparticles heat treated at different temperatures. The evolution of the XRD curves for films containing $\text{Fe}_{55}\text{Pt}_{35}\text{Cu}_{10}$, $\text{Fe}_{48}\text{Pt}_{40}\text{Cu}_{12}$, or $\text{Fe}_{35}\text{Pt}_{50}\text{Cu}_{15}$ nanoparticles was very much the same as Fig. 2. In contrast to the case of films containing $[\text{Fe}_{49}\text{Pt}_{51}]_{88}\text{Ag}_{12}$ nanoparticles,⁷ where the Ag (111) peak appeared as the Ag phase separated for the FePt, there was no new peak at $2\theta = 43.3^\circ$ that could be attributed to the Cu $\langle 111 \rangle$ diffraction. Cu had remained in the particles. However, when heated to high enough temperatures, the films did transform to an $L1_0$ phase as indicated by the appearance of the superlattice peaks $\langle 001 \rangle$ and $\langle 110 \rangle$. In Table I are summarized the unit cell dimensions obtained from the x-ray diffraction data. For all compositions heat treated at 500 °C, there were no superlattice diffraction peaks, indicating the particles remained in the fcc phase. For two of the compositions, $\text{Fe}_{55}\text{Pt}_{35}\text{Cu}_{10}$, and $\text{Fe}_{35}\text{Pt}_{50}\text{Cu}_{15}$, the superlattice peaks appeared after heating at 550 °C, while for the film having $\text{Fe}_{48}\text{Pt}_{40}\text{Cu}_{12}$ and $\text{Fe}_{45}\text{Pt}_{44}\text{Cu}_{11}$ nanoparticles the superlattice peaks appeared after heating at 600 °C.

Earlier we used values of the quotient c/a as a measure of the degree of transformation from the fcc to the $L1_0$ phase for the case of films containing $\text{Fe}_x\text{Co}_y\text{Pt}_{100-x-y}$ nanoparticles.⁶ For the fcc phase the quotient $c/a = 1$ and the quotient decreased to a limiting value as the particles transformed to the $L1_0$ phase—for tetragonal FePt the limiting value is 0.964. Here the quotient c/a also decreases to a limiting value near 0.965 for compositions, $\text{Fe}_{55}\text{Cu}_{35}\text{Cu}_{10}$

TABLE I. Effect of heat treatment temperature on the unit cell dimensions. The degree of tetragonal ordering was quantified by the ratio of the c -axis to the a -axis parameter.

		As-Prepared	500 °C	550 °C	600 °C	700 °C
Fe ₄₈ Pt ₅₂	a (pm)	390	...	385	387	386
	c (pm)	378	376	373
	c/a	1.00	...	0.982	0.972	0.965
Fe ₅₅ Pt ₃₅ Cu ₁₀	a (pm)	384.3	387.7	383.9	389.3	383.9
	c (pm)	376.8	367.2	369.5
	c/a	1.00	1.00	0.989	0.943	0.963
Fe ₄₅ Pt ₄₄ Cu ₁₁	a (pm)	387.0	380.9	380.9	387.3	380.9
	c (pm)	370.5	374.5
	c/a	1.00	1.00	1.00	0.956	0.956
Fe ₄₈ Pt ₄₀ Cu ₁₂	a (pm)	386.4	380.8	382.2	386.8	384.9
	c (pm)	371.3	371.3
	c/a	1.00	1.00	1.00	0.960	0.965
Fe ₃₅ Pt ₅₀ Cu ₁₅	a (pm)	385.7	381.5	385.7	383.9	385.7
	c (pm)	374.3	374.3	369.5
	c/a	1.00	1.00	0.970	0.975	0.958

and Fe₄₈Pt₄₀Cu₁₂, near 0.958 for Fe₄₅Pt₄₄Cu₁₁ and Fe₃₅Pt₅₀Cu₁₅. Values of the unit cell parameters were consistent with a substitutional alloy of FePt containing small amounts of Cu.

Tulameenite (FeCuPt₂) is an iron–platinum–copper mineral from the Tulameen river area of British Columbia.⁸ Tulameenite has a $L1_0$ phase with $a=389.1$ pm, $c=357.7$ pm, and $c/a=0.923$. The ternary Fe–Pt–Cu phase diagram shows a one-phase region for FePtCu and other regions where the $L1_0$ phase and the fcc phase coexist.⁹ Careful examination of the x-ray diffraction curves for the film heat treated at 700 °C (Fig. 2) revealed an extra peak near $2\theta=48.5^\circ$, between the $\langle 200 \rangle$ and the $\langle 002 \rangle$ peaks. This peak may be due to the presence of a small amount of the fcc phase. The extra peak was not seen for Fe₄₈Pt₄₀Cu₁₂.

The coercivities (H_c) of the four FePtCu compositions, along with those of Fe₄₈Pt₅₂, after annealing at temperatures T_a up to 700 °C are listed in Table II. For all compositions,

TABLE II. Effect of heat-treatment temperature of the coercivity of the films, where H_c is the coercivity taken directly from the hysteresis curves, while the values of H_{c1} (soft component) and H_{c2} (hard component) were obtained by decomposing the hysteresis curves.

		500 °C	550 °C	600 °C	700 °C
Fe ₄₈ Pt ₅₂	H_c (Oe)		3,970	6,500	11 600
	H_{c1} (Oe)				
Fe ₅₅ Pt ₃₅ Cu ₁₀	H_c (Oe)	32	518	1,149	3530
	H_{c1} (Oe)				1430
	H_{c2} (Oe)				6800
	H_{c2} (Oe)				10 400
Fe ₄₅ Pt ₄₄ Cu ₁₁	H_c (Oe)	7	105	347	4150
	H_{c1} (Oe)				1330
	H_{c2} (Oe)				10 400
	H_{c2} (Oe)				12 065
Fe ₄₈ Pt ₄₀ Cu ₁₂	H_c (Oe)	11	80	109	8920
	H_{c1} (Oe)				660
	H_{c2} (Oe)				12 065
	H_{c2} (Oe)				12 065
Fe ₃₅ Pt ₅₀ Cu ₁₅	H_c (Oe)	11	20	30	3120
	H_{c1} (Oe)				930
	H_{c2} (Oe)				11 500
	H_{c2} (Oe)				11 500

H_c for the FePtCu particles is significantly less than that of the Fe₄₈Pt₅₂. In addition, the temperature required for significant coercivity enhancement is higher for the particles with copper. This is in sharp contrast to sputtered FePtCu films, in which the coercivity enhancement occurs at much lower temperatures relative to sputtered FePt.

All FePtCu compositions heat-treated at 700 °C showed sheared magnetic hysteresis curves, suggesting a mixture of hard and soft phases. The curves could be decomposed into hard and soft components. The coercivities of the hard and soft components are listed in Table II, along with the coercivities of the full loops. The hard component coercivities of Fe₄₅Pt₄₄Cu₁₁, Fe₄₈Pt₄₀Cu₁₂, and Fe₃₅Pt₅₀Cu₁₅ are all comparable to that of Fe₄₈Pt₅₂. In all cases, the shape of the loops suggests that the maximum field of the AGM is not sufficient to saturate the loops and that the actual coercivities are higher. These results are consistent with the XRD spectra that suggest phase segregation of the FePtCu particles into $L1_0$ and disordered fcc phases. The hysteresis loop for the Fe₄₈Pt₄₀Cu₁₂ particles has the weakest soft magnetic fraction (<20%), which is consistent with the fact that the XRD shows no evidence of a cubic phase. The soft magnetic phases may also consist of iron oxides which, if disordered, would not exhibit well-defined XRD peaks.

For the case of FePt nanoparticles containing Ag, the Ag phase separated from the particles, leaving behind lattice vacancies that allowed the Fe and Pt atoms to move to their $L1_0$ lattice positions at lower temperatures. Here the Cu remained in the FePt lattice to make a FeCuPt alloy, which transformed at higher temperatures to the $L1_0$ phase. Our results were quite different from the results for sputtered FePt films containing Cu, even though we prepared particles with compositions (11%–15% Cu) that gave a strong reduction in the ordering temperature for the sputtered films.⁴ Furthermore, two of the compositions had a nearly 1:1 ratio of Fe to Pt. It is difficult to understand why the results for chemically synthesized FePtCu were different from that for sputtered films. Perhaps, it is the form of the materials as-prepared. Single crystal fcc particles were obtained from the chemical synthesis.

ACKNOWLEDGMENT

This work was supported by the NSF Materials Research Science and Engineering Center Award No. DMR-9809423.

¹S. Sun, C. B. Murray, D. Weller, L. Folks, and A. Moser, *Science* **287**, 1989 (2000).

²D. Weller, A. Moser, L. Folks, M. E. Best, W. Lee, M. F. Toney, M. Schwickert, J. U. Thiel, and M. F. Doerner, *IEEE Trans. Magn.* **36**, 10 (2000).

³Z. R. Dai, S. Sun, and Z. L. Wang, *Nano Lett.* **1**, 443 (2001).

⁴T. Maeda, T. Kai, A. Kikitsu, T. Nagase, and J. Akiyama, *Appl. Phys. Lett.* **80**, 2147 (2002).

⁵Y. K. Takahashi, M. Ohnuma, and K. Hono, *J. Magn. Magn. Mater.* **246**, 259 (2002).

⁶M. Chen and D. E. Nikles, *Nano Lett.* **2**, 211 (2002).

⁷S. Kang, J. W. Harrell, and D. E. Nikles, *Nano Lett.* **2**, 1033 (2002).

⁸L. J. Cabri, D. R. Owens, and J. H. G. LaFlamme, *Can. Mineral.* **12**, 21 (1973).

⁹M. Shahmiri, S. Murphy, and D. J. Vaughan, *Mineralogical Mag.* **49**, 547 (1985).